Analytical Determination of the {Ln – Aminoxyl Radical} Exchange Interaction Taking into Account Both the Ligand-Field Effect and the Spin – Orbit Coupling of the Lanthanide Ion (Ln = Dy^{III} and Ho^{III})

Myrtil L. Kahn,[a] Rafik Ballou,*[b] Pierre Porcher,[c] Olivier Kahn†,[a] and Jean-Pascal Sutter*[a]

This study was performed in conjunction with Professor Olivier Kahn who passed away suddenly on December 8, 1999. This paper is dedicated to his memory.

Abstract: Numerous compounds in which a paramagnetic Ln^{III} ion is in an exchange interaction with a second spin carrier, such as a transition metal ion or an organic radical, have been described. However, except for Gd^{III}, very little has been reported about the magnitude of the interactions. Indeed, for these ions both the ligand-field effects and the exchange interactions between the magnetic centers become relevant in the same temperature range; this makes the analysis of the magnetic behavior of such compounds more difficult. In this study, quantitative analyses of the thermal variations of the static isothermal initial magnetic susceptibility measured on powdered samples of the $\{Ln(NO_3)_3[\text{organic radical}]_2\}$ (Ln = Dy^{III} and Ho^{III}) compounds were performed. The ligand-field effects on the Ln ions were taken into account, and the exchange interactions within a molecule were treated exactly within an appropriate Racah formalism. Values of the intramolecular {Ln – aminoxyl radical} exchange parameter have thus been rigorously deduced for both the Dy Kramers and Ho non-Kramers ion-based compounds. Ferromagnetic {Ln – radical} interactions are found for both the Dy and Ho derivatives with $\boldsymbol{J} = 8\ cm^{-1}$ and $\boldsymbol{J} = 4.5\ cm^{-1}$, respectively.

Keywords: crystal field effect · lanthanides · magnetic properties · orbital momentum · radicals

Introduction

Owing to their rather large and anisotropic magnetic moments, the paramagnetic lanthanide ions have attracted a lot of interest in the field of molecule-based magnetic materials. Such a magnetic anisotropy is required in order to give rise to magnetically ordered materials with large coercive fields, that is, hard magnets. Several compounds in which a Ln^{III} ion is exchange-coupled with a second spin carrier, such as a transition metal ion[1–8] or an organic radical,[9–11] have been described. However, except for the isotropic Gd^{III} ion, which has an $^8S_{7/2}$ ground state, very little is known about the ferro- or antiferromagnetic nature and the magnitude of the interactions in these compounds.

The magnetic properties of a compound in which a paramagnetic Ln^{III} ion interacts with another spin carrier arise from the superposition of two phenomena. One is intrinsic to the Ln ion and originates from the thermal population of the so-called Stark sublevels.[12] The second is the result of the exchange interaction between the magnetic centers. Usually, both become relevant in the same temperature range. For the f-elements, the ligand-field perturbation leads to the splitting of the spectroscopic levels, $^{2S+1}L_J$, of the metal ion. For a $4f^n$ configuration it can result up to $2J+1$ of such Stark sublevels if n is even and $J+1/2$ if n is odd.[12] Generally all the sublevels are populated at room temperature. On decreasing the temperature, the effective magnetic moment of the lanthanide ion will change by thermal depopulation of the Stark sublevels, that is, the magnetic behavior of the Ln ion deviates from Curie behavior. This phenomena is intrinsic to the Ln ion and is modulated by the ligand field and the symmetry of the compound. There is no easy-to-handle analytical model for reproducing this behavior for a given compound. On the other hand, for a lanthanide ion, the correct quantum number

[a] Dr. J.-P. Sutter, M. L. Kahn, Prof. Dr. O. Kahn†
Institut de Chimie de la Matière Condensée de Bordeaux
UPR CNRS N° 9048, 33608 Pessac (France)
Fax: (+33) 5-56-84-26-49
E-mail: jpsutter@icmcb.u-bordeaux.fr

[b] Dr. R. Ballou
Laboratoire Louis Néel, CNRS
B.P. 166, 38042 Grenoble (France)
Fax: (+33) 4-76-88-11-91
E-mail: ballou@labs.polycnrs-gre.fr

[c] Dr. P. Porcher
Laboratoire Chimie Appliquée du Solide, UMR 7574
Ecole Nationale Supérieure de Chimie, 75231 Paris (France)

  0947-6539/02/0802-0525 $ 17.50+.50/0

is the total angular momentum, J_{Ln}, while the exchange interaction involves solely the spin momentum S_{Ln}. A quantitative treatment of this interaction will then require the use of Racah algebra, all the more as the ligand-field effects on the Ln ion may lead to the mixing of multiplets and spectral terms. This makes the analysis of the magnetic behavior of compounds for which a Ln^{III} ion with a first-order orbital momentum is exchange coupled with another spin carrier more difficult.

Recently, we described an experimental approach that provided access to qualitative information on whether the {Ln^{III}–aminoxyl radical} interaction is ferro- or antiferromagnetic. The magnetic properties of a series of compounds, {$Ln(NO_3)_3$[organic radical]$_2$}, comprising a Ln^{III} ion (Ln = Ce to Ho) surrounded by two N,O-chelating aminoxyl radicals have been investigated.[13, 14] The experimental approach used to get insight into the {Ln–radical} coupling occurring within these compounds is based on the knowledge of the intrinsic paramagnetic contribution of the metal ion. For each compound, this contribution has been deduced from the corresponding {$Ln(NO_3)_3$[nitrone]$_2$} derivative in which the Ln^{III} ion is now in a diamagnetic environment. The difference

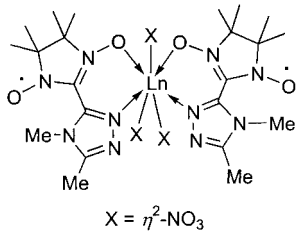

{$Ln(NO_3)_3$[organic radical]$_2$}

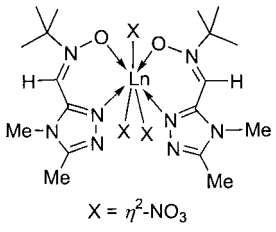

{$Ln(NO_3)_3$[nitrone]$_2$}

between the magnetic susceptibility of the {$Ln(NO_3)_3$[organic radical]$_2$} compound and the corresponding {$Ln(NO_3)_3$[nitrone]$_2$} derivative then permits the ferro- or antiferromagnetic nature of the correlation within the {$Ln(NO_3)_3$[organic radical]$_2$} compounds to be established. For Ln = Ce, Pr, Nd, and Sm antiferromagnetic interactions have been found. Conversely, ferromagnetic interactions were observed for Ln = Gd, Tb, Dy, and Ho. Assuming that Hund's rules dominate the ligand-field effects on the Ln ions, this would suggest that the {Ln–aminoxyl radical} spin–spin exchange interaction is always ferromagnetic.

Our experimental method led to qualitative information about the nature of the interactions and has established the importance of the ligand-field effect in the overall magnetic behavior of these compounds. In order to go one step further, we addressed the problem of quantitative evaluation of the exchange interaction, taking into account the ligand-field effect. This paper describes our approach and the results obtained for the {$Dy(NO_3)_3$[organic radical]$_2$} and {$Ho(NO_3)_3$[organic radical]$_2$} compounds, respectively a Kramers and a non-Kramers Ln ion derivative.

Model and formalism: The exchange interactions in the {$Ln(NO_3)_3$[organic radical]$_2$} compounds are much weaker than the ligand-field effects on the Ln ion. There was, thus, no need to simultaneously diagonalize the corresponding Hamiltonians. The approach we followed to analyze the magnetic behavior of {$Dy(NO_3)_3$[organic radical]$_2$} and {$Ho(NO_3)_3$[organic radical]$_2$}, consisted, then, of two steps. First, the ligand-field effect, that is, the intrinsic contribution of the rare earth ion, was modeled in order to determine the energy diagram $\{E_{Ln}\}$ of the Stark sublevels for the Ln ions and the associated eigenfunctions $\{|\Psi_{Ln}>\}$. Then the exchange interactions were computed in the tensorial product space $\{|\Psi_{Ln}> |S_{Rad1}>|S_{Rad2}>\}$ of the state functions $|\Psi_{Ln}>$ of the Ln ion in its ligand-field environment with the state functions $|S_{Rad1}>$ and $|S_{Rad2}>$ of the two radicals with which the Ln ion interacts by exchange.

The ligand-field effect: As mentioned above, the first step of our approach consisted of computing the spectrum of the low-lying states of the Ln ion in its ligand-field environment. Interestingly, both magnetic and optical properties of the Ln ions have their origin in the spectroscopic Stark sublevels. Analytical models of the ligand field exist that describe the optical properties of these ions in different materials and that can be adapted to compute the spectrum of the low-lying states of the Ln compounds considered here.

In this study we used the *semiempirical* simple overlap model (SOM).[15] This model has been successfully applied to calculating the crystal-field parameters (CFPs) over a wide variety of Ln^{III} compounds in single-crystal or polycrystalline forms.[16] In these compounds, the point symmetry of the site occupied by the rare earth ion ranged from the high cubic O_h to the very low C_2 symmetries. This model assumes that the interaction energy of a Ln ion in a chemical environment is produced by an electrostatic potential of charges uniformly distributed over small regions centered around the mid-point of the R distance from the Ln ion to the ligand, the charge in each region being proportional to the total overlap integral ρ between the 4f and the s and/or p orbitals of the ion and the ligand, respectively. The CFPs are written as below.

$$B_q^k = \langle r^k \rangle \sum_\mu \rho_\mu \left(\frac{2}{1 \pm \rho_\mu} \right)^{k+1} A_q^k(\mu)$$

$$\rho_\mu = \rho_O \left(\frac{R_O}{R_\mu} \right)^{3.5}$$

The sum over μ is restricted to the ligands of the first coordination sphere, and thus $\langle r^k \rangle$ radial integrals[17] are not corrected from the spatial expansion. ρ varies for each ligand as a function of the distance R, according to the exponential law above indicated, R_0 being the shortest distance. For the rare earth ions $0.05 \leq \rho \leq 0.08$. A_q^k is the lattice sum and it takes into account the symmetry properties of the Ln^{III} ion site, including the effective charge attributed to the ligand. The sign $\pm$ of the denominator stands for differentiating the type of ligand. When a single type of ligand is considered, a minus sign should be taken, which corresponds to the normal shift of the charge barycenter from the mid-point of the R bonding distance. When different ligands are present, the minus sign corresponds to the most covalent one. Finally, only three parameters have to vary, that is, the overlap ρ and the

0947-6539/02/0802-0526 $ 17.50+.50/0 *Chem. Eur. J.* **2002**, *8*, No. 2

effective charges q_O and q_N for the oxygen and nitrogen ions, respectively.

In the present case all free ion parameters have been set to the standard values given by Carnall[18] and the CFPs are those derived from SOM calculation. When the secular determinant of the configuration has been diagonalized,[18] the eigenfunctions are those considered for calculating the paramagnetic susceptibility, by using the van Vleck formula.[19]

In order to reproduce as precisely as possible the effective contribution of the Ln ion, ρ, q_O, and q_N have been tuned in order to fit the calculated magnetic susceptibility curve to the experimental $\chi_{Ln}T$ curve obtained for the $\{Ho(NO_3)_3[nitrone]_2\}$ compound, in which Ho is in a diamagnetic environment. Indeed, the magnetic behavior of a Ln(nitrone) derivative corresponds to the χ_{Ln} contribution of the Ln ion in the $\{Ln(NO_3)_3[organic\ radical]_2\}$ compound.[13, 14] The Ho derivative was chosen because the magnetic susceptibility of this ion shows a strong thermal variation between the low- and high-temperature domains. The reproduction of such a pronounced temperature dependence will ensure that the ligand field is accurately modeled. In Figure 1, the experimental curve is compared to the best calculated curve with

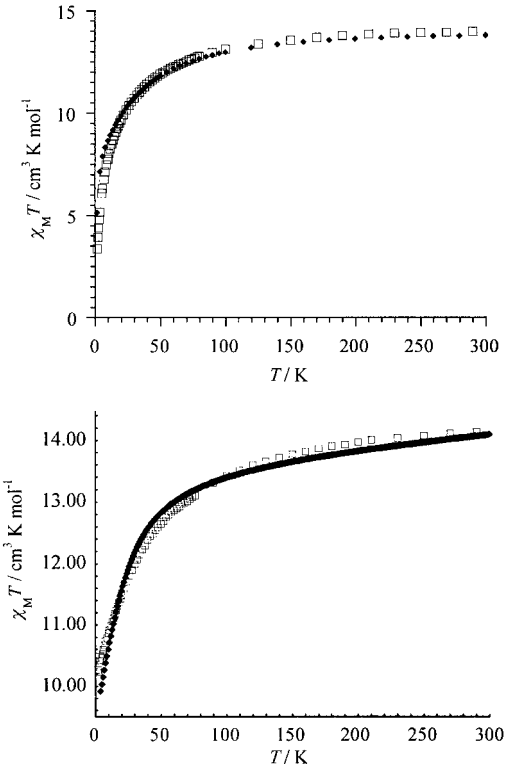

Figure 1. Top: Experimental (□) and calculated (◆) temperature dependence of $\chi_{Ln}T$ for the $\{Ho(NO_3)_3[nitrone]_2\}$ compound. Bottom: Related curves for $\{Dy(NO_3)_3[nitrone]_2\}$

effective charges of -1.4 and -0.7 for N and O, respectively, and an overlap parameter $\rho_0 = 0.08$. The corresponding eigenfunctions and eigenvalues were computed by taking into account all spectroscopic terms and multiplets of the Ho ion. The same parameter set allowed the $\chi_{Ln}T$ versus T curve of the related Dy(nitrone) compound to be well reproduced (Inset Figure 1) and was used to calculate the eigenfunctions and eigenvalues corresponding to the isomorphous $\{Dy(NO_3)_3[organic\ radical]_2\}$ compound. Previous calculations performed on several Dy^{III} and Ho^{III} compounds have shown that the crystal-field parameter set for a given ligand-field environment remains very similar for these ions.[20, 21] These eigenfunctions and eigenvalues were used for the analyses of the {Ln – organic radical} exchange interactions.

The exchange interaction: The topology of the $\{Ln(NO_3)_3[organic\ radical]_2\}$ compounds in terms of exchange interactions is shown in Figure 2. Two interactions have to be considered.

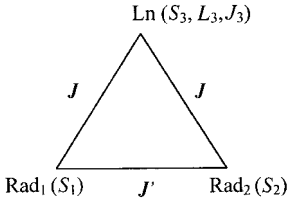

Figure 2. Schematic representation of the exchange interactions.

One is the exchange interaction between the Ln^{III} ion and the organic radical, $\boldsymbol{J}$, and the second is the intramolecular exchange interaction between the two organic radicals, $\boldsymbol{J'}$. Indeed, for $\{La(NO_3)_3[organic\ radical]_2\}$ in which La is a diamagnetic ion, an antiferromagnetic interaction was found between the two paramagnetic ligands.[11] This radical – radical interaction has been taken into account in our analytical model.

The exchange Hamiltonian, H_{ex}, corresponding to the topology described in Figure 2 is given by Equation (1).

$$H_{ex} = -\boldsymbol{J}\vec{S}_{Ln}\cdot(\vec{S}_{rad1} + \vec{S}_{rad2}) - J'\vec{S}_{rad1}\cdot\vec{S}_{rad2} \quad (1)$$

In this expression $\vec{S}_{Ln}$, $\vec{S}_{rad1}$, and $\vec{S}_{rad2}$ are the spin quantum numbers of the Ln^{III} ion and of the two radicals, respectively ($S_{rad1} = S_{rad2} = ½$). As already noted above, an exchange interaction only takes place between spin momenta. The susceptibility measurements have been performed with an applied field; therefore, the Zeeman effect must also be taken into account [Eq. (2)].

$$\begin{aligned} H_z = &-\mu_B\vec{B}\cdot(\vec{L}_{Ln} + g_e\vec{S}_{Ln}) - \mu_B\vec{B}\cdot(g_e\vec{S}_{rad1} + g_e\vec{S}_{rad2}) \\ &- N < (\vec{L}_{Ln} + g_e\vec{S}_{Ln}) + (g_e\vec{S}_{rad1} + g_e\vec{S}_{rad2}) > \cdot[(\vec{L}_{Ln} + g_e\vec{S}_{Ln}) + (g_e\vec{S}_{rad1}) + g_e\vec{S}_{rad2})] \end{aligned} \quad (2)$$

In this Hamiltonian, H_Z, the first and second terms correspond to the Zeeman effect that acts on the total angular momentum of each paramagnetic species present in the system (one lanthanide ion and two organic radicals). The third term corresponds to the intermolecular interactions introduced in the mean field approximation.

The matrix elements of the $H_{ex} + H_Z$ Hamiltonian [Eq. (3)] were calculated in the tensorial product space $\{|\Psi_{Ln}> |S_{rad1}> |S_{rad2}>\}$ of the state functions of the Ln ion in its ligand-field environment with those of the two radicals.

$$<\Psi_{Ln}|<S_{rad1}|<S_{rad2}|H_{ex} + H_z|\Psi_{Ln}>|S_{rad1}>|S_{rad2}> \quad (3)$$

The state functions of the Ln ion are naturally and best described in the $\{|\xi, S_{Ln}, L_{Ln}, J_{Ln}, M_J>\}$ multiplet representation. We recall that the intra-atomic electron correlation discriminates between the states of the Ln ion in terms of total spin momentum, S_{Ln}, and total orbital momentum, L_{Ln}, which would lead to the $\{|\xi, S_{Ln}, M_S, L_{Ln}, M_L>\}$ spectral term representation. However, owing to the spin–orbit coupling the M_S and M_L quantum numbers cease to be appropriate, and the correct quantum numbers for a Ln ion in a spherically symmetric environment are then the total angular momentum, J_{Ln}, and its component, M_J, along a given quantization axis.

Both the H_{ex} and H_Z Hamiltonian incorporate operators acting either on the spin momentum, S_{Ln}, or on the orbital momentum, L_{Ln}, of the Ln ion, but never they act on the total angular momentum J_{Ln}. In the case in which the ligand field does not induce multiplets ($J'-J$) or spectral term ((L',S')–(L,S)) mixing, the matrix elements of the S_{Ln} and L_{Ln} operators in the $H_{ex} + H_Z$ Hamiltonian [Eq. (4)] are easily evaluated, within the ground-state multiplet, in terms of effective gyromagnetic ratios by making use of the Wigner–Eckart theorem.

$$<\Psi_{Ln}|H_{ex}+H_z|\Psi_{Ln}> = <\xi',S_{Ln}',L_{Ln}',J_{Ln}',M_J'|H_{ex}+H_Z|\xi,S_{Ln},L_{Ln},J_{Ln},M_J> \quad (4)$$

Unfortunately, the ligand field on the Ln ions in the $\{Ln(NO_3)_3[\text{organic radical}]_2\}$ compounds gives rise to non-negligible multiplets and spectral-term mixing. Consequently, to calculate the matrix elements of the $H_{ex} + H_Z$ Hamiltonian [Eq. (4)], the more complex formalism described by Judd[22] has to be used. In fact, the main problem arises from the evaluation of the matrix elements between states of different S_{Ln}, L_{Ln}, and J_{Ln} quantum numbers, of the components with respect to a given system of axis, of the spin momentum [Eq. (5)] and of the orbital momentum [Eq. (6)] of the Ln ion.

$$<\xi',S_{Ln}',L_{Ln}',J_{Ln}',M_J'|\mathbf{S_{Ln}}|\xi,S_{Ln},L_{Ln},J_{Ln},M_J> \quad (5)$$

$$<\xi',S_{Ln}',L_{Ln}',J_{Ln}',M_J'|\mathbf{L_{Ln}}|\xi,S_{Ln},L_{Ln},J_{Ln},M_J> \quad (6)$$

The formalism described by Judd allows the matrix elements $<\gamma',j_1',j_2',J',M'|X|\gamma,j_1,j_2,J,M>$ to be calculated; here X is an operator (Hamiltonian) acting on both j_1 and j_2 but not on J.[22] In other words, X is an operator formed from two operators, each of which acts on two different parts of the system, namely j_1 and j_2. By using the Wigner–Eckart theorem, the matrix element $<\gamma',j_1',j_2',J',M'|X|\gamma,j_1,j_2,J,M>$ can be express as a function of the reduced matrix element $<\gamma',j_1',j_2',J',\|X\|\gamma,j_1,j_2,J>$. Judd has described how to calculate this reduced matrix element.[22] In our specific case, two types of matrix elements [Eq. (5) and Eq. (6)] have to be considered. By using the Judd formalism these are determined, respectively, by Equation (7) and Equation (8) as functions of the 3*j* and 6*j* symbols.

$$<\xi SLJM|L_q|\xi'S'L'J'M'> = \delta(\xi,\xi')\delta(S,S')\delta(L,L')(-1)^{J-M}(-1)^{S+L+J+1}\begin{pmatrix} J & 1 & J' \\ -M & q & M' \end{pmatrix} \sqrt{(2J+1)(2J'+1)}\sqrt{L(L+1)(2L+1)}\begin{Bmatrix} J & 1 & J' \\ L & S & L \end{Bmatrix} \quad (7)$$

$$\langle\xi SLJM|S_q|\xi'S'L'J'M'\rangle = \delta(\xi,\xi')\delta(S,S')\delta(L,L')(-1)^{J-M}(-1)^{S+L+J'+1}\begin{pmatrix} J & 1 & J' \\ -M & q & M' \end{pmatrix} \sqrt{(2J+1)(2J'+1)}\sqrt{S(S+1)(2S+1)}\begin{Bmatrix} J & 1 & J' \\ S & L & S \end{Bmatrix} \quad (8)$$

Once these matrix elements had been evaluated, the $H_{ex} + H_z$ Hamiltonian could be diagonalized in the tensorial product space $\{|\Psi_{Ln}>|S_{rad1}>|S_{rad2}>\}$. Although the ligand field on the Ln ion gives rise to multiplets and spectral term mixing, the SOM calculations showed that the effect is not large enough to completely destroy the multiplet structure of the spectrum. The energy levels of the Ln ion in the ligand-field environment group themselves in terms of pseudo-multiplets. In particular, the lowest energy pseudo-multiplet, for both Ho and Dy, is well separated in energy from the rest of the spectrum by one order of magnitude with respect to the lowest energy pseudo-multiplet total splitting. The $H_{ex} + H_z$ Hamiltonian was thus actually diagonalized not in the whole $\{|\Psi_{Ln}>|S_{rad1}>|S_{rad2}>\}$ space but in the restricted space defined by limiting the $\{|\Psi_{Ln}>|\}$ states to belonging solely to the lowest energy pseudo-multiplet. The advantage was, of course, the gain in both computing memory storage and central processor unit time for diagonalization and subsequent calculations of thermodynamic properties. Calculations in a larger space of states, including several pseudo-multiplets, were performed. Corrections were found to be very weak and not at all relevant.

Various thermodynamic quantities, magnetization, specific heat, etc. could be computed from the new *eigenvalues* $\{E_p\}$ and associated *eigenfunctions* $\{|p>\}$ obtained after diagonalization of the $H_{ex} + H_z$ Hamiltonian. Our experimental measurements concerned the static isothermal magnetic susceptibility χ_M of powdered samples. This was calculated by using the linear response theory.[23–25] By writing M_i, the component of the magnetic moment operator $\vec{M} = \mu_B[(\vec{L}_{Ln} + g_e\vec{S}_{Ln}) + g_e(\vec{S}_{rad1} + g_e\vec{S}_{rad2})]$ along an axis *i* of a system of cartesian axes (x,y,z), the static isothermal initial magnetic susceptibility tensor, χ_{ij}^T, is given in Equation (9).

$$\chi_{ji}^T = -\frac{\mu_B^2}{Z_0}\sum_p e^{-\beta E_p}\sum_{\substack{q \\ E_q\neq E_p}}\frac{1}{E_p-E_q}(M_{i_{pq}}M_{j_{qp}}+M_{j_{qp}}M_{j_{pq}}) + \frac{\mu_B^2}{Z_0}\beta\sum_p e^{-\beta E_p}\sum_{\substack{q \\ E_q=E_p}}M_{i_{pq}}M_{j_{qp}} - \frac{\mu_B^2}{Z_0^2}\beta\sum_p e^{-\beta E_p}\sum_{\substack{q \\ E_q=E_p}}M_{i_{pq}}\sum_q e^{-\beta E_p}\sum_{\substack{q \\ E_q=E_p}}M_{j_{qp}}, \quad (9)$$

Here $M_{i_{pq}}=<p|M_i|q>$ and $M_{j_{pq}}=<p|M_j|q>$ are the matrix elements of the operators M_i and M_j. $Z_0 = \sum_p \exp(-\beta E_p)$ is the partition function under zero applied field. The molar magnetic susceptibility, χ_M, at a given temperature $T = 1/\beta k_B$ was deduced from χ_{ij}^T by averages over all the crystal orientations inherent to a powdered sample.

Numerical fitting: In order to evaluate the exchange interaction between the radicals, we first determined the $\boldsymbol{J'}$ parameter for the $\{La(NO_3)_3[\text{organic radical}]_2\}$ compound by our computer program. For this compound, only the two radical ligands contribute to the magnetic behavior, La^{III} being diamagnetic. The best calculated $\chi_M T$ versus T curve was obtained for $\boldsymbol{J'} = -6\ cm^{-1}$ (Figure 3). This antiferromag-

0947-6539/02/0802-0528 $ 17.50+.50/0 *Chem. Eur. J.* **2002**, *8*, No. 2

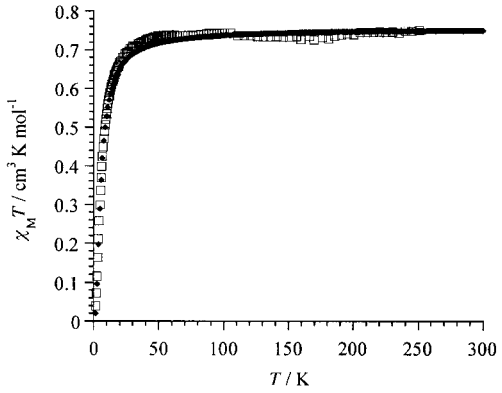

Figure 3. Experimental (□) $\chi_{Ln}T$ versus T behavior for {La(NO$_3$)$_3$[organic radical]$_2$} and calculated curve (◆) obtained for $J' = -6$ cm^{-1}.

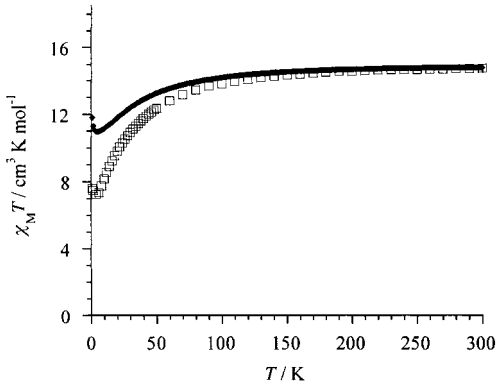

Figure 5. Experimental (□) $\chi_{Ln}T$ versus T behavior for {Ho(NO$_3$)$_3$[organic radical]$_2$} and calculated curve (◆) obtained for $\boldsymbol{J} = 4.5$ cm^{-1}, $\boldsymbol{J}' = -6$ cm^{-1} (fixed).

netic exchange-parameter value corresponds to the value found previously for this compound by the van Vleck formula for two interacting $S = 1/2$ spins.[11] A very close $\boldsymbol{J}'$ parameter has been found for the corresponding Gd^{III} compound.[11] Consequently, we decided to fix the value of this parameter to $\boldsymbol{J}' = -6$ cm^{-1} for the subsequent simulations of the magnetic behavior of the Dy and Ho compounds. Moreover, results we obtained previously for the Gd^{III} derivative, {Gd(NO$_3$)$_3$-[organic radical]$_2$}, have shown that the intermolecular interaction $\boldsymbol{J}''$ is in the order of 10^{-2} cm^{-1}, at least two orders of magnitude smaller than the intramolecular interactions $\boldsymbol{J}$ and $\boldsymbol{J}'$. For this reason we decided to fix $\boldsymbol{J}'' = 0$ for the computations.

The best simulated curve obtained for {Dy(NO$_3$)$_3$[organic radical]$_2$} is compared to the experimental $\chi_M T$ versus T curve in Figure 4. The calculated curve was obtained for $\boldsymbol{J} = 8$ cm^{-1} and $\boldsymbol{J}' = -6$ cm^{-1} (fixed). It reproduces well the features of the

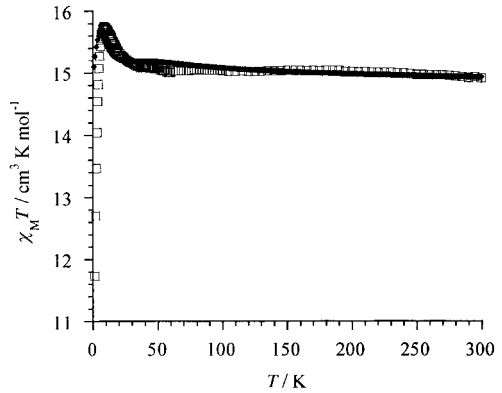

Figure 4. Experimental (□) $\chi_{Ln}T$ versus T behavior for {Dy(NO$_3$)$_3$[organic radical]$_2$} and calculated curve (◆) obtained for $\boldsymbol{J} = 8$ cm^{-1}, $\boldsymbol{J}' = -6$ cm^{-1} (fixed).

experimental data especially the maximum in $\chi_M T$ at 7 K, which is observed experimentally at 10 K. For the {Ho-(NO$_3$)$_3$[organic radical]$_2$} compound, the best-simulated behavior was obtained for $\boldsymbol{J} = 4.5$ cm^{-1} and $\boldsymbol{J}' = -6$ cm^{-1} (fixed). This curve is compared to the experimental data in Figure 5. The calculated curve presents the same features as the experimental one. As the temperature is lowered, $\chi_M T$ decreases to reach a small minimum at about 4 K and then increases for lower temperatures. However, whereas the shape and features of the two curves in Figure 5 are the same, a difference exists for their relative values of $\chi_M T$ and this difference is more pronounced in the low temperature range. No improvement was obtained when an intermolecular contribution, $\boldsymbol{J}''$, was considered as well. Attempts to optimize the simulated curve by tuning both $\boldsymbol{J}$ and $\boldsymbol{J}'$ did not lead to better results. Of course, by slightly increasing the contribution of these parameters, it was possible to bring the simulated curve down to the experimental data, but to the detriment of the characteristic minimum. For this reason, we considered the curve shown in Figure 4 to be the best simulation, with the minimum at the same temperature as the experimental curve.

The interaction parameters found for both the Dy and Ho derivatives indicate that in these compounds the {Ln – aminoxyl} interaction is ferromagnetic. These analytical results are in agreement with those found previously in our phenomenological approach.[14]

Discussion

The accurate analysis of the magnetic behavior of a molecular compound containing a Ln^{III} ion that displays spin – orbit coupling and is in exchange interaction with another spin carrier requires the intrinsic contribution arising from the Ln^{III} ion to be properly taken into account. All the energy sublevels of the Ln ion involved in the investigated temperature range have to be considered in order to determine the exchange parameter. This is the approach we followed to analyze the magnetic behavior of the {Dy(NO$_3$)$_3$[organic radical]$_2$} and {Ho(NO$_3$)$_3$[organic radical]$_2$} compounds. Interaction parameters, $\boldsymbol{J}$, of 8.0 and 4.5 cm^{-1} have thus been found for the {Dy-aminoxyl} and {Ho-aminoxyl} interaction, respectively. In both cases, a ferromagnetic {Ln – organic radical} interaction was obtained, in agreement with the qualitative study.[14]

The site symmetry of the Ln ion in the {Ln(NO$_3$)$_3$[organic radical]$_2$} compounds is C_1, the lowest symmetry. Consequently, for a Kramers $4f^n$ ion (n odd), the number of expected Stark sublevels is $J+½$ and these are doubly degenerate. On the other hand, for a non-Kramers ion (n even), the number of

sublevels should be $2J+1$. The energy diagrams of the Stark sublevels determined by SOM for the Dy^{III} and Ho^{III} compounds, respectively $4f^9$ and $4f^{10}$ ions, are depicted in Figure 6. The degeneracy expected for both ions is well reproduced. It can be seen that for Ho^{III}, the ground Stark sublevel is just 5 K below the first excited state, whereas for

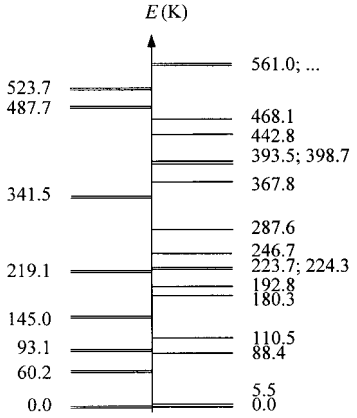

Figure 6. Energy diagrams of the Stark sublevels for $\{Dy(NO_3)_3[organic\ radical]_2\}$ and $\{Ho(NO_3)_3[organic\ radical]_2\}$ determined by SOM.

Dy^{III}, the ground and first excited states are separated by about 60 K. This small difference in energy between the states of the Ho ion may account for the difficulty in exactly reproducing the ligand-field effect by SOM at low temperature, and consequently, perfectly reproducing the magnetic behavior of the $\{Ho(NO_3)_3[organic\ radical]_2\}$ compound. Indeed, any small inaccuracy in the lowest levels of the energy diagram of the Stark sublevels will have a substantial effect on the calculated $\chi_M T$ versus T behavior of the {Ho-aminoxyl} compound, especially in the lower temperature range. This is exactly what is observed in Figure 5, in which a deviation between the experimental and calculated curves appears at low temperature. We attribute the differences between the experimental and calculated data to the difference between the effective and calculated thermal population of the lowest states. This difference is the result of the small error made on computing the energy splitting of these levels. Nevertheless, as can be seen in Figure 5, the general feature of the experimental curve is perfectly reproduced by the analytical simulation. This indicates that the exchange parameters, J and J', used for the computation reflect the interactions occurring in the compound well. The problem encountered with Ho does not apply to Dy^{III}. For this ion, the first excited sublevel is much higher in energy. The magnetic behavior of the $\{Dy(NO_3)_3[organic\ radical]_2\}$ compound could be well reproduced by computation down to low temperature (Figure 4). Intermolecular interactions have not been taken into account in the reported computations. For the related Gd^{III} derivative, these intermolecular interactions were found to be very small ($-0.009\ cm^{-1}$), and no appreciable modification was observed when J'' was taken as different to zero for the computations.

The ferromagnetic interactions found for the {Dy–aminoxyl}, $J = 8\ cm^{-1}$, and {Ho-aminoxyl} compounds, $J = 4.5\ cm^{-1}$, compare well with the ferromagnetic interaction, $J = 6.1\ cm^{-1}$, found previously for the related Gd^{III} derivative. These three compounds being isomorphous, the variations observed for the $\boldsymbol{J}$ parameters may be directly related to the Ln ions. Apparently, the strengths of the exchange interaction follow the effective moment of the Ln^{III} ion at low temperature. For the Ln(nitrone) derivatives of Dy and Ho, these were found to equal 11.1 $cm^3 K mol^{-1}$ (9.4 μ_B) and 3.4 $cm^3 K mol^{-1}$ (5.2 μ_B), respectively, at 2 K.

Conclusion

We quantitatively analyzed the magnetic behavior of $\{Ln(NO_3)_3[organic\ radical]_2\}$ compounds in which the Ln ion, characterized by its $\{|\xi, S_{Ln}, L_{Ln}, J_{Ln}, M_J>\}$ multiplet structure associated with electron correlation and spin–orbit coupling, is in a ligand-field environment and interacts by exchange with two organic radicals. The ligand-field effect was considered within the SOM and the {Ln–radical} and {radical–radical} exchange interactions were treated exactly. The numerical fits to the experimental static isothermal magnetic susceptibility χ_M measured on powdered samples allowed the {Ln–radical} and {radical–radical} exchange parameters for the Ho and Dy derivatives to be quantitatively determined.

Some discrepancies exit between the experimental and calculated thermal variation of χ_M that can be ascribed to the limitations of the SOM on evaluating the ligand-field effects. The very low site symmetry (C_1) of the Ln ion in the $\{Ln(NO_3)_3[organic\ radical]_2\}$ compounds leads to a large number of crystal-field parameters, and it would clearly be illusory to let them vary freely and fit them solely from the variations of χ_M. Improvements can be expected from fitting to measurements of the magnetization vector on single crystals, as the full static isothermal initial magnetic susceptibility tensor, χ_{ij}^T can be obtained from this. Quasi-elastic and inelastic neutron scattering on powdered samples should also be very useful, as this would allow the magnetic energy levels of the molecules to be accurately determined, provided deuterated samples are used to avoid the strong incoherent neutron scattering from hydrogen. In order to isolate the magnetic signals from the neutron scattering by phonons, measurements with polarized neutrons and polarization analysis should be performed. Another interesting measurement would be that of the magnetic density by polarized neutron-scattering measurements on a single crystal. This magnetic density can be computed from the eigenstates $\{|p>\}$ of the molecules.[26] Evidently, all these experimental measurements will essentially allow the knowledge of the ligand-field effects to be improved beyond the SOM. We do not expect drastic changes in the values of the exchange parameters we have obtained.

We would finally like to emphasize that in order to quantitatively estimate the intramolecular exchange parameters in the $\{Ln(NO_3)_3[organic\ radical]_2\}$ compounds with sufficient confidence, the formalism we have worked out is absolutely necessary. Actually, any compound that has an ion with a first-order orbital momentum, in a ligand-field environment and in exchange interaction with another spin

  0947-6539/02/0802-0530 $ 17.50+.50/0 *Chem. Eur. J.* **2002**, *8*, No. 2

carrier should rigorously be treated in the same way. Our computer program can be generalized for any such molecules.

Acknowledgement

Financial support was partly provided by the TMR Research Network ERBFMRXCT-980181 of the European Union, entitled "*Molecular Magnetism*, *from Materials towards Devices*".

[1] T. Sanada, T. Suzuki, S. Kaizaki, *J. Chem. Soc. Dalton Trans.* **1998**, 959.
[2] M. Andruh, O. Kahn, J. Sainton, Y. Dromzee, S. Jeannin, *Inorg. Chem.* **1993**, *32*, 1623.
[3] J.-P. Costes, F. Dahan, A. Dupuis, J.-P. Laurent, *Chem. Eur. J.* **1998**, *4*, 1616.
[4] J.-P. Costes, A. Dupuis, J.-P. Laurent, *J. Chem. Soc*, *Dalton Trans.* **1998**, 735.
[5] S. Decurtins, M. Gross, H. W. Schmalle, S. Ferlay, *Inorg. Chem.* **1998**, *37*, 2443.
[6] X.-M. Chen, Y.-L. Wu, Y.-Y. Yang, S. M. J. Aubin, D. N. Hendrickson, *Inorg. Chem.* **1998**, *37*, 6186.
[7] M. L. Kahn, C. Mathoniere, O. Kahn, *Inorg. Chem.* **1999**, *38*, 3692.
[8] M. L. Kahn, T. M. Rajendiran, Y. Jeanin, C. Mathonnière, O. Kahn, *C. R. Acad. Sci. Paris*, *Série IIc* **2000**, 131.
[9] C. Benelli, A. Caneschi, D. Gatteschi, R. Sessoli, *Inorg. Chem.* **1993**, *32*, 4797.
[10] P. L. Jones, A. J. Amoroso, J. C. Jeffery, J. A. McCleverty, E. Psillakis, L. H. Rees, M. D. Ward, *Inorg. Chem.* **1997**, *36*, 10.
[11] J. P. Sutter, M. L. Kahn, L. Ouahab, O. Kahn, *Chem. Eur. J.* **1998**, *4*, 571.
[12] J. C. G. Bünzli, G. R. Chopin in *Lanthanide Probes in Life*, *Chemical and Earth Sciences*: *Theory and Practice*, Elsevier, Amsterdam, **1989**.
[13] J.-P. Sutter, M. L. Kahn, O. Kahn, *Adv. Mater.* **1999**, *11*, 863.
[14] M. L. Kahn, J.-P. Sutter, S. Golhen, P. Guionneau, L. Ouahab, O. Kahn, D. Chasseau, *J. Am. Chem. Soc.* **2000**, *122*, 3413.
[15] O. L. Malta, S. J. L. Ribeiro, M. Faucher, P. Porcher, *J. Phys. Chem. Solids* **1991**, *52*, 587.
[16] P. Porcher, M. Couto dos Santos, O. Malta, *Phys. Chem. Chem. Phys.* **1999**, *1*, 397.
[17] A. J. Freeman, J. P. Desclaux, *J. Magn. Magn. Mater.* **1979**, *12*, 11.
[18] W. T. Carnall, G. L. Goodman, K. Rajnak, R. S. Rana, *J. Chem. Phys.* **1989**, *90*, 3443.
[19] C. Cascales, R. Saez Puche, P. Porcher, *J. Alloys Compd.* **1998**, *275 – 277*, 384.
[20] J. Holsa, R. J. Lamminmaki, M. Lastusaari, P. Porcher, R. S. Puche, *J. Alloys Compd.* **2000**, *300*, 45.
[21] J. Holsa, R. J. Lamminmaki, M. Lastusaari, E. P. Chukalina, M. N. Popova, P. Porcher, *J. Lumines.* **2000**, *87 – 89*, 1052.
[22] B. R. Judd, *Operator Techniques in Atomic Spectroscopy*, McGraw – Hill, New York, **1963**.
[23] R. Kubo, *J. Phys. Soc. Jpn.* **1957**, *12*, 570.
[24] G. V. Chester, *Rep. Prog. Phys.* **1963**, *26*, 411.
[25] R. Kubo, *Rep. Prog. Phys.* **1966**, *29*, 255.
[26] W. Marshall, S. W. Lovesey, *Theory of Thermal Neutron Scattering*, Clarendon, Oxford, **1971**.

Received: May 23, 2001
Revised: September 26, 2001 [F3280]